A Multiobjective Approach to the Management of Opt-In Distributed Energy Resources

Shu Tu
Lehigh University
Bethlehem, PA 18015
Email: sht213@lehigh.edu

Boris Defourny
Lehigh University
Bethlehem, PA 18015
Email: defourny@lehigh.edu

Somayeh Moazeni
Stevens Institute of Technology
Hoboken, NJ 07030
Email: smoazeni@stevens.edu

***Abstract*—This paper considers the problem of coordinating Distributed Energy Resources (DERs) in a radial distribution work below a substation, in order to meet an injection schedule at the substation. Loads, dispatchable resources, nondispatchable resources, and energy storage are modeled in the problem. Uncertainty in load and nondispatchable generation is considered using scenarios. The focus is on situations where there are many identical agents willing to participate, but only a subset of them can be scheduled, due to network congestion. A multiobjective approach is proposed, where the first objective is chosen to promote the equity of network access among agents over time, and the second objective is concerned with the control of the overall deviation from the injection schedule. A fundamental tradeoff is to determine the extent to which generation is provided from non-dispatchable resources, and the level of risk of deviation from the schedule that can be tolerated. Simulations are used to illustrate the tradeoff between the objectives, and assess the level of nondispatchable resources that can be integrated.**

***Index Terms*—Coordination of Distributed Energy Resources, Grid Access, Equity, Mixed-Integer Second-Order Cone Optimization**

NOMENCLATURE

n	Index for the agent in $1,\dots,N$.
t	Index for the time period in $1,\dots,T$.
k	Index for the realization of random variables.
b	Bus index in $1,\dots,B$.
ℓ	Line index in $1,\dots,L$.
$\bar{d}_t$	Committed power by a Load Serving Entity.
p_{nt}	Power injected by agent n at time t.
$\mathcal{N}$	The set $\{1,\dots,N\}$, with subsets defined below.
$\mathcal{N}^D$	Index set for loads.
$\mathcal{N}^G$	Index set for dispatchable generation.
$\mathcal{N}^W$	Index set for nondispatchable generation.
$\mathcal{N}^X$	Index set for energy storage resources.

I. INTRODUCTION

Increased coordination is a necessary condition to the development of distributed energy resources (DERs) [1]. A variety of coordination schemes, enabled by IT advances [2], have been proposed to create virtual power plants [3], perform demand response [4], demand-side management [5], voltage management [6]. See [7] for a review of demand response programs implemented in the US.

DER coordination can be implemented by a load serving entity (LSE), which can be distinct from the utility. Fostering the coordination between DERs and utilities has long been an objective of Integrated Resource Planning (IRP) [8].

Important and possibly conflicting criteria the LSE has to simultaneously take into account for the design of a load management mechanism include (i) revenue adequacy, (ii) economic efficiency, and (iii) equitable treatment of users. In particular (iii) means that the LSE should ensure, and be able to transparently report, equitable treatment among the users, especially when some users are able transact over the distribution network while others see their resource being curtailed or mitigated. With the advent of energy storage, the utilization of nearby energy storage resources adds to the panoply of actions the LSE may take to optimize the access to the distribution grid resources.

Transmission system operators (TSOs) have long faced similar requirements. For instance, in the US, the Open Access Same-Time Information System (OASIS) organizes access to transmission. Differentiated treatment of users is still unavoidable, for instance when the TSO needs to force subsets of generating units to shutdown and others to be online independently of the market price in effect at the bus locations. Often TSOs have resorted to ex-post side payments settled out of the market.

However, the side-payment mechanism leaves open the problem of selecting the participants allowed to operate. At the level of the distribution grid, issues would be compounded by the potentially large number of very similar users. Besides the litigation risk, already pervasive at the TSO level [9], the perception that the mitigation system is not equitable could ultimately hamper investment in DERs.

The present paper introduces a load serving entity problem formulation that schedules the power injection of users and gives grid access with equity considerations directly built into the formulation. Concretely, the geometric mean is used as the device to aggregate a cumulated utility function assigned to each user by the LSE, subject to the constraints of the distribution grid. Arguably, other mathematical devices are possible: axiomatic descriptions of fairness measures have been studied in [10]. The geometric mean retains two essential benefits: while remaining easy to explain to users, it can be tractably optimized (owing to second-order cone optimization representation).

The paper is organized as follows. Section II formulates the LSE problem. Sec. III describes the distribution grid approximation for this paper. Sec. IV reports on simulations used to evaluate the proposed mechanism on a radial distribution network model featuring a mix of dispatchable and nondispatchable resources. Finally, Sec. V concludes.

II. Load Serving Entity Problem

The perspective of a load serving entity (LSE) is adopted. The LSE is assumed to have committed to inject power at a substation, according to a schedule described by $\bar{d}_t$, $t = 1, \ldots, T$. The LSE utilizes the net power produced by the distributed generation below the substation to realize the injection schedule.

The LSE is tasked with preparing a multiobjective injection schedule. Three high-level objectives are identified:

1) Limiting the penalties for the LSE incurred by deviations from the committed schedule.
2) Leveraging the capacity of DERs (dispatchable generation, nondispatchable generation, energy storage).
3) Ensuring that opt-in participants remain satisfied of the LSE actions in the long-run.

As the revenue adequacy requirement suggests that the penalties will be paid back by network users, all participants are assumed to be willing to reveal their best predictions.

A. Controlling Penalties

To describe the first objective, let $\widetilde{d}_t$ denote the power injected into the external grid from the substation, and let $\widetilde{\epsilon}_t = \widetilde{d}_t - \bar{d}_t$ denote the excess injected power. Let $\ell_t : \mathbb{R} \mapsto \mathbb{R}$ be a nonnegative convex function, with $\ell_t(0) = 0$, representing the expected penalty for deviating from the committed injection $\bar{d}_t$.

At the time of scheduling, several possible realizations ϵ_t^k of $\widetilde{\epsilon}_t$ are envisioned,

$$\epsilon_t^k = d_t^k - \bar{d}_t, \tag{1}$$

detailed in the sequel. Then, the first objective is handled as a constraint, by imposing

$$\ell_t(\epsilon_t^k) \leq \bar{\ell}_t, \quad \text{for all } k, t. \tag{2}$$

Essentially, the LSE sets the bounds $\bar{\ell}_t$ on the maximum acceptable deviation penalty at each time step, and verifies the bounds hold for all considered scenarios. Then with high confidence (depending on the choice of the scenarios), the total deviation penalty is kept below

$$\bar{\ell}^{\text{tot}} = \textstyle\sum_{t=1}^{T} \bar{\ell}_t.$$

The relation between the power d_t^k injected at the substation and the quantities p_{nt}^k injected by the agents $n \in \mathcal{N}$ depends on the network model and the injection points. Additional constraints exist such as the need for keeping flows and voltage levels within bounds. This is described in §III. If all the production and consumption at the substation was lumped (no network, no losses), one would simply have $d_t^k = \sum_{n \in \mathcal{N}} p_{nt}^k$.

B. Scheduling Distributed Generation

Distributed generation comes in two varieties. Agents $n \in \mathcal{N}^G$ have dispatchable generation (such as gas-fueled units controlled by the LSE). Their production profile is described by $p_{n1}, \ldots, p_{nT}$. The agents $n \in \mathcal{N}^W$ have nondispatchable generation (such as renewables). Their nondispatchable production $\widetilde{p}_{nt}$ is known to lie in the interval $[\bar{p}_{nt}^0, \bar{p}_{nt}^1]$.

The LSE decides which agent is allowed to operate at time t, using binary decision variables $b_{nt} \in \{0, 1\}$ and the following constraints for $k = 0, 1$ which refers to the two scenarios $k = 0, 1$ and their associated adapted variables,

$$p_{nt}^k = \bar{p}_{nt}^k b_{nt}, \qquad n \in \mathcal{N}^W \tag{3}$$

$$P_n^{\min} b_{nt} \leq p_{nt}^k \leq P_n^{\max} b_{nt}, \qquad n \in \mathcal{N}^G. \tag{4}$$

Loads are treated as nondispatchable, uncurtailable negative injections, using

$$p_{nt}^k = \bar{p}_{nt}^k, \qquad n \in \mathcal{N}^D, \tag{5}$$

where $\bar{p}_{nt}^0 \leq \bar{p}_{nt}^1 < 0$ determine the possible range of withdrawn power.

Essentially, the LSE prepares a schedule for two scenarios: Scenario $k = 0$ where all nondispatchable resources produce at their minimum and loads maximally consume, and Scenario $k = 1$ where all nondispatchable resources produce at their maximum and loads minimally consume. The schedule for dispatchable resources is adapted to the scenario.

C. Scheduling Energy Storage

The agents $n \in \mathcal{N}^X$ correspond to dispatchable energy storage resources. For each agent $n \in \mathcal{N}^X$ we define

x_{nt}	Withdrawn power by charging at period t.
y_{nt}	Injected power by discharging at period t.
$P_n^{\max}$	Power rating.
c_{nt}	Energy level at the beginning of period t.
$c_n^{\min}, c_n^{\max}$	Range of operation for the energy level.
$\eta_n^{\text{ch}}, \eta_n^{\text{dis}}$	Charging and discharging efficiency, in [0,1].

Let δ_t be the duration of period t. The injected power and energy level change during period t, in scenario $k = 0, 1$ (see §II-B) are described as

$$p_{nt}^k = y_{nt}^k - x_{nt}^k, \tag{6}$$

$$c_{n,t+1}^k - c_{nt}^k = (x_{nt}^k / \eta_n^{\text{ch}} - y_{nt}^k \eta_n^{\text{dis}}) \delta_t, \qquad n \in \mathcal{N}^X. \tag{7}$$

The capacity constraints for all t are

$$0 \leq x_{nt}^k \leq b_{nt}^{X,k} P_n^{\max}, \tag{8}$$

$$0 \leq y_{nt}^k \leq b_{nt}^{Y,k} P_n^{\max}, \tag{9}$$

$$c_n^{\min} \leq c_{nt}^k \leq c_n^{\max}, \tag{10}$$

$$b_{nt}^{X,k} + b_{nt}^{Y,k} \leq b_{nt}, \qquad n \in \mathcal{N}^X. \tag{11}$$

The objective optimized in the sequel cannot ensure that at the optimum, x_{nt}^k and y_{nt}^k are not simultaneously positive. Therefore, binary variables $b_{nt}^{X,k}$ and $b_{nt}^{Y,k}$ are used to enforce this constraint, at the same time that the binary variable b_{nt} indicates if storage operations are allowed at all at time t.

D. Ensuring Equitable Access to the Distribution Grid

Similar opportunities of being able to transact over the distribution grid are given by the LSE to the DERs by maximizing the following objective,

$$\begin{aligned}
\text{maximize} \quad & \min_{k=0,1} \left[\prod_{n=1}^{N} \left(1+U_n^k\right)\right]^{1/N} && (12)\\
\text{subject to} \quad & U_n^k = \textstyle\sum_{t=1}^{T} u_{nt}^k, && n \in \mathcal{N}, \quad (13)\\
& u_{nt}^k = 0, && n \in \mathcal{N}^D, \quad (14)\\
& u_{nt}^k \le u(p_{nt}^k), && n \in \mathcal{N}^G, \quad (15)\\
& u_{nt}^k \le u(p_{nt}^k), && n \in \mathcal{N}^W, \quad (16)\\
& u_{nt}^k = 0, && n \in \mathcal{N}^X, \quad (17)
\end{aligned}$$

where $u(\cdot)$ is a nonnegative increasing concave utility function, defined on the nonnegative real line with $u(0) = 0$, assigned to each DER by the LSE. The variable u_{nt}^k represents the utility of resource n at time t consecutive to a possible transaction p_{nt}^k under scenario k. The variable U_n^k represent the cumulative utility over the scheduling horizon.

Resorting to the geometric mean contrasts with usual welfare maximization approaches for optimal dispatch. The geometric mean tends to allocate the same value to each U_n^k, while the concavity of $u(\cdot)$ encourages the uniform spreading of the contributions p_{nt}^k among a maximal number of entities n.

E. Computational Tractability

The geometric mean $[\prod_{n=1}^{N} \left(1+U_n^k\right)]^{1/N}$ is jointly concave in U_n^k, $n \in \mathcal{N}$, see e.g. Example 3.14 in [11]. The minimum of concave functions is concave, thus the objective is concave. The concavity of $u(\cdot)$ ensures that the inequality constraints where $u(\cdot)$ is involved are convex.

The geometric mean admits a second-order cone (SOC) representation, which can be found e.g. in [12], §2.3. Thus if $u(\cdot)$ also admits a second-order cone representation, the optimization problem can be solved by commercial solvers such as cplex/gurobi/mosek, which handle mixed-integer second-order cone optimization problems (MISOCOs).

Examples of SOC-representable functions $u(\cdot)$ include:

- Linear utility function: $u(p) = ap$ with $a > 0$. This leads to the representation $u_{nt}^k \le ap_{nt}^k$.
- Power utility with rational power: $u(p) = p^{r/s}$ where $0 < r < s$ are integer. This leads to a geometric-mean representation $0 \le u \le (\prod_{i=1}^{s} z_i)^{1/s}$, $z_i = p$ for $i = 1, \dots, r$, $z_i = 1$ for $i = r+1, \dots, s$, itself being SOC-representable. In our experiments in §IV, $u(p) = \sqrt{p}$.

Relating back to §II-B, it is important to realize that in the absence of constraints linking successive time steps, the schedule b_{nt} computed by taking into account the two extreme scenarios $(k = 0, 1)$ ensures the satisfaction of all constraints on any mixed scenario made by switching between scenario $k = 0$ and scenario $k = 1$ any number of times during the planning horizon. The presence of storage units along with Constraint (7) introduces temporal dependence, but the extent to which this could damage the robustness of the schedule to mixed scenarios could arguably remain relatively limited.

We also note that the scenarios are defined such that that the variations are perfectly correlated among units. This is highly plausible given the exposure to the same local weather-induced variations.

III. Distribution Grid

In our simulation for this paper we employ a linear DC power flow approximation, described in §III-A. First, we describe some general notation.

N	# of agents (cardinality of $\mathcal{N}$).
n_B, n_L	# of buses and lines in the network representation.
n_D, n_G, n_W, n_X	# of loads, dispatchable units, nondispatchable units, and storage units.
b	Bus index in $1, \dots, n_B$.
ℓ	Line index in $1, \dots, n_L$.
R_ℓ^{A}	A-rating of line ℓ.
A	Bus incidence matrix in $\{0,1\}^{n_B \times N}$.

The grid below the substation (a.k.a. distribution feeder) has n_B buses and n_L lines. The high-voltage side of the transformer of the substation, connected to the transmission grid, is used as the reference bus. The line ratings are collected in the vector $R^{\text{A}} \in \mathbb{R}^{n_L}$. The bus incidence matrix is a 0-1 matrix such that $A_{bn} = 1$ if agent $n \in \mathcal{N}$ is located at bus b, and 0 otherwise.

It is convenient to also define a bus incidence matrix A^{out} as the n_b-dimensional row vector with 1 as the first element and zero otherwise, to locate the point of power withdrawal by the external grid.

A. Linear DC Power Flow Approximation

The DC network approximation is not recommended when the ratio R/X from branch impedances $Z_\ell = R_\ell + \mathrm{j}\, X_\ell$ is not small. Nevertheless, define

p_t^{inj}	Power injected at buses at time t, in $\mathbb{R}^{n_B}$.
p_t	Power injected by agents at time t, in $\mathbb{R}^{N}$.
F_t	Vector of branch flows at time t, in $\mathbb{R}^{n_L}$.
H	Power transfer distribution factor (PTDF) matrix in $\mathbb{R}^{n_L \times n_B}$.

The PTDF matrix is calculated with the substation as the reference bus. $H_{\ell b}$ represents the incremental power flowing through line ℓ consecutive to an incremental injection of 1 kW at bus b combined with a withdrawal of 1 kW at the reference bus. Under the DC power flow approximation, the branch flows and capacity constraints are expressed as

$$p_t^{\text{inj}} = Ap_t - A^{\text{out}} d_t, \tag{18}$$

$$F_t = Hp_t^{\text{inj}}, \tag{19}$$

$$1^\top p_t^{\text{inj}} = 0, \tag{20}$$

$$-R^{\text{A}} \preceq F_t \preceq R^{\text{A}}. \tag{21}$$

The flows should be calculated for the two scenarios $k = 0, 1$, thus in fact in place of $p^{\text{inj}}, p_t, F_t, d_t$ we use the variables $p^{\text{inj},k}, p_t^k, F_t^k, d_t^k$.

IV. SIMULATIONS

Simulations are carried out on a radial 8-bus test system. The line diagram of this system is presented in Fig. 1(a). The optimization problem consists in maximizing the objective (12), for the $N = 26$ agents of the system (as detailed below), subject to the constraints (1) to (11) and (13) to (21). The input data are described in §IV-A. Some of the data, such as the load profiles (Fig. 1(c) described below), are adapted from EPRI's OpenDSS project [13].

A. Description of the Test System

There are $n_G = 7$ dispatchable generation units labeled G1 to G7. Their placement is indicated on the diagram. Each unit has $P_n^{\min} = 5$ and $P_n^{\max} = 20$ in (4).

There are also $n_W = 11$ nondispatchable generation units labeled W1 to W11. Their placement is indicated on the diagram. Fig. 1(b) indicates the 2 possible production levels ($k = 0$, $k = 1$) that are possible at any period of the day for each of those units.

There are $n_L = 6$ loads, placed at each bus below the substation, that is, all buses except buses 1 and 4. The load is different at each bus, and has 2 possible levels ($k = 0$, $k = 1$). A base consumption profile $\bar{p}_{nt}^{\text{base}}$, adapted from load shapes taken from OpenDSS, is depicted in Fig. 1(c). The load profile is multiplied by a factor 0.8 or by 1.2 to obtain the load levels $\bar{p}_{nt}^k$ at each bus.

The system has $n_X = 2$ storage units labeled ST1 and ST2. Their placement is indicated on the diagram of Fig. 1(a). Their parameters are $P_n^{\max} = 2.5$, $c_n^{\min} = 0$, $c_n^{\max} = 5$, and $\eta_n^{\text{ch}} = \eta_n^{\text{dis}} = 0.9$.

Thus in total, there are $N = 26$ agents.

Given the radial topology and the use of a lossless DC network approximation, the PTDF matrix is independent of the impedances of the lines, hence the impedance data can be omitted from the description. The rating of the lines for the maximum flows (in per unit) is as follows. Line 3-6: 300. Lines 4-1, 2-7, 7-8: 250. Line 8-4: 90. Line 5-4: 30.

B. Cases

The LSE has committed to an injection schedule $\bar{d}_t$ for $t = 1, \ldots, 24$, see the black line in Figures 2(c) and 3(c).

The penalties for deviation are such that the realized injection $\widetilde{d}_t$ must remain in the interval $[\bar{d}_t - \Delta, \bar{d}_t + \Delta]$ where Δ is a parameter of the case instance. This implicitly defines the function ℓ_t of equation (2). In Case 1, we assume $\Delta = 0.1$. In Case 2, we assume $\Delta = 10$. These maximal deviations are indicated by the outer rectangles depicted in Figures 2(c), 3(c) (the inner gray rectangles describe the solution described in §IV-D).

Essentially, the main tradeoff for the LSE is the quantity of nondispatchable generation, versus the predictability of injections. This tradeoff translates into a curtailment plan of select nondispatchable units in advance. Within the margins for injection, the LSE sets up a schedule such that the dispatchable units and storage units can balance the variations from the load and noncurtailed nondispatchable generation.

As mentioned in §II-E, the utility function that the LSE assigns to each generating unit is $u(p) = \sqrt{p}$, that is, each generator is treated equally, and the utility grows with the injected power, but less than proportionally, to express the preference towards solutions that split a target production level into a larger number of generators.

C. Solver Settings

We use Mosek as the solver, and run the codes on a pc equipped with a 2.80GHz Intel Xeon processor.

There is a high degree of symmetry in our test system. The goal indeed is to investigate the tie-breaking properties of solutions obtained via the formulation proposed in this paper.

In unit commitment problems with a "traditional" cumulative objective function, symmetry among generators is known to impede on getting a tight duality gap certificate, and possibly create oscillations among equivalent solutions, see e.g. [14], [15]. Therefore, in our simulations, wallclock time is used as the stopping criterion, and a limit of 120 seconds is set for all problem instances.

D. Results

Details of the solutions are reported in Fig. 2 for Case 1, and Fig. 3 for Case 2.

Figures 2(a) and 3(a) describe the curtailment decisions for the nondispatchable resources.

A first observation is that the solution with $\Delta = 0.5$ curtails all nondispatchable units with more intensity than the solution with $\Delta = 10$, which is expected given the tighter tolerance asked from the schedule.

A second observation is that the curtailment decisions are well spread out among all nondispatchable units. While it cannot be ruled out that better solutions could be found by letting the solver work longer, it can already be observed that the variance of the number of periods a resource is curtailed is smaller in Case 2. This is expected, given that the goal of staying close to the committed schedule is given less importance by the choice of Δ.

Figures 2(b) and 3(b) describe the status of the dispatchable resources. There are two groups, that correspond to the branching after the substation. The number of periods with nonzero output is more uniform among the units of the first group G1-G2-G3 in Case 2.

Figures 2(c) and 3(c) describe the commitments (black line), the maximum deviation Δ around the commitment (outer rectangles), and the range of injection determined by the two extreme scenarios $k = 0, 1$ (gray rectangle).

The cumulated utilities of each generator for the two scenarios and the two cases are reported in Table I. The last row of Table I reports the geometric mean of the corresponding column (shifted by 1), GMean=$[\prod_{n \in \mathcal{N}^G \cup \mathcal{N}^W} (1 + U_n^k)]^{\frac{1}{18}}$. Recall that the cumulated utility of demand and storage are set to 0, so the geometric means that include these contributions are maximized by the same solutions. The smallest GMean among the two scenarios is the one being maximized and is typeset in bold.

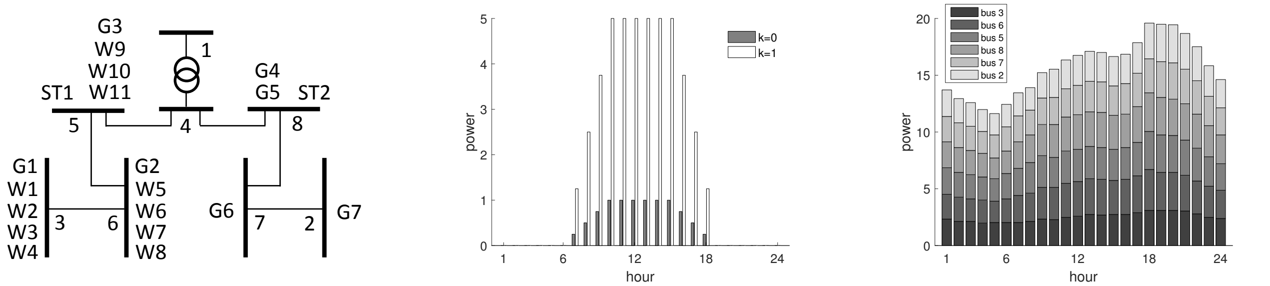

(a) Line diagram & DERs placement

(b) Power profiles $\bar{p}^k_{nt}$, $k = 0, 1$, in Eq. (3) for nondispatchable generators W…

(c) Power profile $\bar{p}^{\text{base}}_{nt}$ for load, such that $\bar{p}^0_{nt} = -1.2\bar{p}^{\text{base}}_{nt}$ and $\bar{p}^1_{nt} = -0.8\bar{p}^{\text{base}}_{nt}$ in Eq. (5)

Fig. 1. 8-bus Test System comprised of 7 dispatchable generators G…, 11 nondispatchable units W…, and 2 storage units ST…

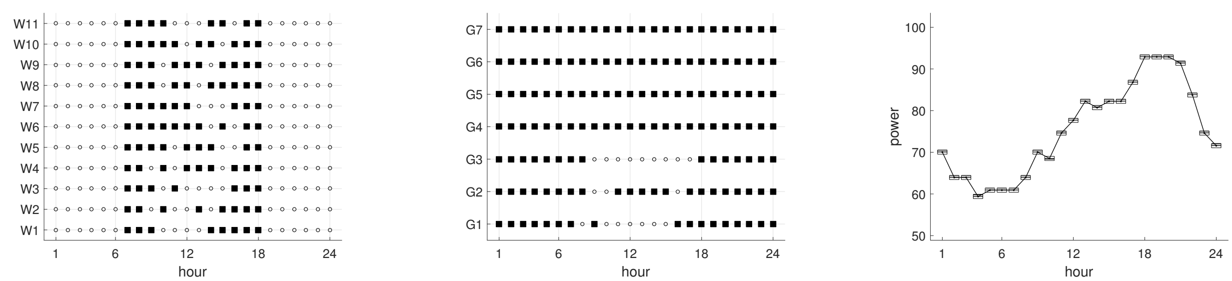

(a) Binary decisions b_{nt} for $n \in \mathcal{N}^W$

(b) Binary decisions b_{nt} for $n \in \mathcal{N}^G$

(c) Commitment $\bar{d}_t$ and realization bounds.

Fig. 2. Solution to Case 1, that has the injection schedule tolerance set to $\Delta = 0.5$. In Figs 2(a), 2(b): Black square: $b_{nt} = 1$, White circle: $b_{nt} = 0$. In Fig 2(c), Black line: Commitment $\bar{d}_t$; Outer rectangle: Bounds $\bar{d}_t \pm \Delta$ to control deviation penalties; Inner gray rectangle: Deviation bounds of the schedule.

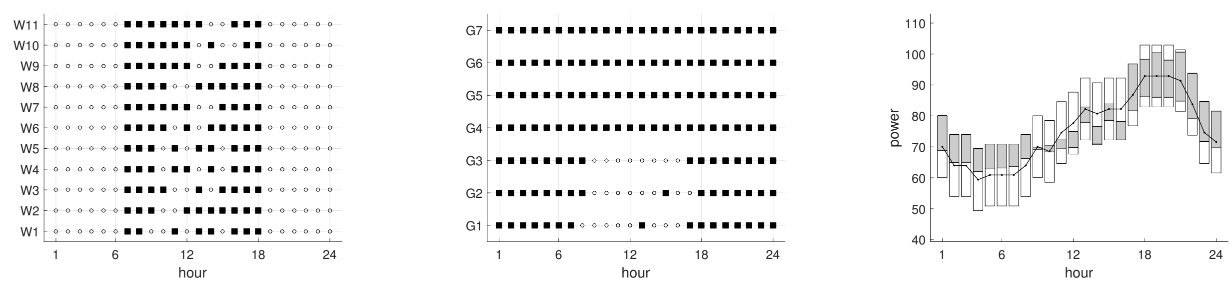

(a) Binary decisions b_{nt} for $n \in \mathcal{N}^W$

(b) Binary decisions b_{nt} for $n \in \mathcal{N}^G$

(c) Commitment $\bar{d}_t$ and realization bounds.

Fig. 3. Solution to Case 2: $\Delta = 10$.

V. Discussion and Concluding Remarks

The simulations of §IV suggest that the geometric mean formulation is functioning as intended, resulting in an effort to make individual schedules as comparable to others as possible. Larger deviations to the committed schedule appear to offer more opportunities to make individual schedules similar.

The formulation that has been proposed controls the maximum deviation to a schedule, and the worst geometric mean of a cumulative utility for each agent. The actual cumulative utility will depend on the realization of the nondispatchable resources. It is good to keep in mind that agents can be compensated for the power they provide, independently of the choice of the utility function used for their selection, and that the actual penalties for the actual deviation from the schedule should be allocated ex-post among the agents.

As pointed out by a reviewer, in a distribution system, the uncertainty and variation is high compared with a transmission system. In the present work, feasibility is ensured by allowing a smaller subset of non-dispatchable resources to participate. However, this is expected to raise equity concerns among the agents, which may ultimately discourage agents from participating. In the present paper, the objective function acts as a device to alternate among non-dispatchable resources that are scheduled.

Figures 2(a) and 3(a) in particular show that all resources of this type tend to suffer from a very similar number of

TABLE I
CUMULATED UTILITIES U_n^k.

Unit	Case I		Case II	
	U_n^0	U_n^1	U_n^0	U_n^1
W1	7.15	11.46	6.28	10.36
W2	7.15	11.75	8.15	13.10
W3	8.15	13.11	7.15	11.75
W4	7.15	11.76	7.15	11.75
W5	7.15	11.76	7.15	11.75
W6	5.41	9.43	8.15	13.21
W7	8.15	13.29	8.15	13.21
W8	8.15	13.29	8.15	13.21
W9	5.41	9.43	8.15	13.21
W10	6.28	10.79	7.28	12.19
W11	8.15	13.42	8.15	13.35
G1	64.55	36.59	59.34	36.21
G2	74.54	40.28	59.27	36.17
G3	59.76	34.51	59.13	35.84
G4	92.80	49.89	99.08	50.90
G5	92.81	47.77	99.09	49.15
G6	92.81	47.77	99.09	49.15
G7	92.81	49.95	99.09	51.14
GMean	**19.78**	20.66	**20.53**	21.40

curtailments, placed at different time periods. Comparing the two figures, equity seems higher for the plan in Figure 3(a). However, this is achieved at the cost of allowing for potentially higher deviations from the schedule, as indicated by the gray rectangles in Figure 3(c), which cover the set of possible realizations.

In the same vein of results, Table I reports on the utility of each agent, for the two extreme scenarios $k = 0$ and $k = 1$. The proposed approach focuses on the utility for the worst outcome, which turns out to be the scenario $k = 0$ in both cases. In case I there is still a discrepancy between the utility of W6, equal to 5.41, to be compared to the utility 8.15 that other identical agents enjoy on this the schedule. The discrepancy is somehow less pronounced in case II, with W1 receiving only 6.28 while other similar agents get 8.15.

It is expected, however, that over time, the objective can be used to balance the discrepancies among the agents created by individual schedules. Concretely, in (12), the factor $1 + U_n^k$ can be changed to $c + U_n^k$, where c is used to summarize the utility received from past schedules.

ACKNOWLEDGMENT

This material is based upon work supported by the National Science Foundation under Grants No. 1610825 and 1610302.

REFERENCES

[1] F. Rahimi and A. Ipakchi, "Demand response as a market resource under the smart grid paradigm," *IEEE Trans. Smart Grid*, vol. 1, no. 1, pp. 82–88, 2010.

[2] Z. Fan, P. Kulkarni, S. Gormus, C. Efthymiou, G. Kalogridis, M. Sooriyabandara, Z. Zhu, S. Lambotharan, and W. H. Chin, "Smart grid communications: Overview of research challenges, solutions, and standardization activities," *IEEE Communications Surveys Tutorials*, vol. 15, no. 1, pp. 21–38, 2013.

[3] P. Lombardi, M. Powalko, and K. Rudion, "Optimal operation of a virtual power plant," in *2009 IEEE Power Energy Society General Meeting*, 2009, pp. 1–6.

[4] J. Medina, N. Muller, and I. Roytelman, "Demand response and distribution grid operations: Opportunities and challenges," *IEEE Trans. Smart Grid*, vol. 1, no. 2, pp. 193–198, 2010.

[5] I. Atzeni, L. G. Ordonez, G. Scutari, D. P. Palomar, and J. R. Fonollosa, "Demand-side management via distributed energy generation and storage optimization," *IEEE Trans. Smart Grid*, vol. 4, no. 2, pp. 866–876, 2013.

[6] E. Yao, P. Samadi, V. W. S. Wong, and R. Schober, "Residential demand side management under high penetration of rooftop photovoltaic units," *IEEE Trans. Smart Grid*, vol. 7, no. 3, pp. 1597–1608, 2016.

[7] "Assessment of demand response and advanced metering," Federal Energy Regulatory Commission, Tech. Rep., december 2016. [Online]. Available: https://www.ferc.gov/legal/staff-reports/2016/DR-AM-Report2016.pdf

[8] E. Hirst and C. Goldman, "Creating the future: Integrated resource planning for electric utilities," *Annual Review of Energy*, vol. 16, no. 1, 1991.

[9] "Viridity Energy, Inc. versus PJM Interconnection, L.L.C." 2016, docket No. EL12-54-000.

[10] T. Lan, D. Kao, M. Chiang, and A. Sabharwal, *An axiomatic theory of fairness in network resource allocation*. IEEE, 2010.

[11] S. Boyd and L. Vandenberghe, *Convex Optimization*. Cambridge University Press, 2004.

[12] M. Lobo, L. Vandenberghe, S. Boyd, and H. Lebret, "Applications of second-order cone programming," *Linear Algebra and its Applications*, vol. 284, pp. 193–228, 1998.

[13] R. Dugan and T. McDermott, "An open source platform for collaborating on smart grid research," in *2011 IEEE Power and Energy Society General Meeting*, July 2011, pp. 1–7.

[14] Q. Zhai, X. Guan, and J. Cui, "Unit commitment with identical units: Successive subproblem solving method based on Lagrangian relaxation," *IEEE Trans. Power Systems*, vol. 17, no. 4, pp. 1250–1257, 2002.

[15] J. Alemany, F. Magnago, D. Moitre, and H. Pinto, "Symmetry issues in mixed integer programming based unit commitment," *International Journal of Electrical Power & Energy Systems*, vol. 54, pp. 86–90, 2014.